Polar Opposites: Erk Direction of CD4 T Cell Subsets

Chiung-Fang Chang, Warren N. D'Souza, Irene L. Ch'en, Gilles Pages, Jacques Pouyssegur and Stephen M. Hedrick

J Immunol 2012; 189:721-731; Prepublished online 6 June 2012;
doi: 10.4049/jimmunol.1103015
http://www.jimmunol.org/content/189/2/721

The Journal of Immunology is published twice each month by The American Association of Immunologists, Inc., 9650 Rockville Pike, Bethesda, MD 20814-3994.

Print ISSN: 0022-1767 Online ISSN: 1550-6606.

Polar Opposites: Erk Direction of CD4 T Cell Subsets

Chiung-Fang Chang,* Warren N. D'Souza,† Irene L. Ch'en,* Gilles Pages,‡ Jacques Pouyssegur,‡ and Stephen M. Hedrick*

Effective immune responses depend upon appropriate T cell differentiation in accord with the nature of an infectious agent, and the contingency of differentiation depends minimally on TCR, coreceptor, and cytokine signals. In this reverse genetic study, we show that the MAPK Erk2 is not essential for T cell proliferation in the presence of optimum costimulation. Instead, it has opposite effects on T-bet and Gata3 expression and, hence, on Th1 and Th2 differentiation. Alternatively, in the presence of TGF-β, the Erk pathway suppresses a large program of gene expression, effectively limiting the differentiation of Foxp3$^+$ regulatory T cells. In the latter case, the mechanisms involved include suppression of *Gata3* and *Foxp3*, induction of *Tbx21*, phosphorylation of Smad2,3, and possibly suppression of Socs2, a positive inducer of Stat5 signaling. Consequently, loss of Erk2 severely impeded Th1 differentiation while enhancing the development of Foxp3$^+$-induced T regulatory cells. Selected profiles of gene expression under multiple conditions of T cell activation illustrate the opposing consequences of Erk pathway signaling. ***The Journal of Immunology*****, 2012, 189: 721–731.**

The differentiation of T cells in response to infectious agents constitutes an essential step in effective immune responses. Minimally, Ag-stimulated T cells can take on one of four programs of cytokine production and effector function: IFN-γ–secreting Th1 cells effective against viruses and intracellular microbes, IL-4–secreting Th2 cells most effective against helminths, IL-17–secreting Th17 cells effective against extracellular microbes, and induced regulatory T cells (iTregs) that limit inflammation and autoimmunity (1). These differentiation programs are engaged in response to cytokines and the conditions of Ag presentation, but the T cell-intrinsic signaling pathways that are operative are not entirely understood.

The signaling pathway from membrane-bound receptors to the activation of Erk is found in every cell type in metazoan species. Erk interacts with many substrates and regulators to modulate signal transduction in the cytoplasm, as well as to program gene expression in the nucleus (2, 3). It constitutes a highly connected node in the matrix of cell signaling. The effects include cell-cycle progression, lineage specification and cellular differentiation, survival, chemotaxis, learning and memory, and the elaboration of cell-type–specific functions.

*University of California, San Diego, La Jolla, CA 92093-0377; †Amgen Inc., Thousand Oaks, CA 91320; and ‡Institute of Developmental Biology and Cancer Research, University of Nice Sophia-Antipolis, Centre National de la Recherche Scientifique, Unité Mixte de Recherche 6543, Antoine Lacassagne Center, 06189 Nice, France

Received for publication October 21, 2011. Accepted for publication May 10, 2012.

This work was supported by National Institutes of Health Grant 5RO1AI021372-27 (to S.M.H.).

The gene expression profiles presented in this article have been submitted to Gene Expression Omnibus (http://www.ncbi.nlm.nih.gov/geo/) under accession number GSE37554.

Address correspondence and reprint requests to Dr. Stephen M. Hedrick, Molecular Biology Section, University of California, San Diego, 5121 NSB, 9500 Gilman Drive, La Jolla, CA 92093-0377. E-mail address: shedrick@ucsd.edu

The online version of this article contains supplemental material.

Abbreviations used in this article: iTreg, induced regulatory T cell; LCMV, lymphocytic choriomeningitis virus; qPCR, quantitative real-time PCR; Treg, regulatory T cell; UCSD, University of California, San Diego; WT, wild-type.

www.jimmunol.org/cgi/doi/10.4049/jimmunol.1103015

The two Erk isoforms appear to act additively in cell cycle control (4); a loss of *Erk1* (*Mpk3*) function reveals few phenotypic changes, whereas even a hemizygous loss of *Erk2* (*Mpk1*) causes embryonic lethality in some strains of mice (5–8). The origin of *Erk2* loss-of-function lethality was due, in part, to failure of the polar trophectoderm cells to proliferate (6). In several other physiological models there are differential requirements for Erk1 and Erk2 that do not correlate with dramatic differences in the relative amounts of Erk1 and Erk2 expressed (9).

The strength of signal through the TCR influences the outcome of differentiation; a strong and prolonged Erk signal gave rise to Th1 cells, whereas weak Ag stimulation or an attenuation of Erk gave rise to IL-2–dependent Stat5 phosphorylation, Gata3 expression, and IL-4 production (10, 11). Alternatively, an inhibitor of the Erk kinases, Mek1,2, was found to enhance Foxp3 expression and regulatory T cell (Treg) differentiation (12, 13). In this study, we used genetic ablation of Erk1 or Erk2 to study the T cell-intrinsic role of this pathway in proliferation, expansion, and differentiation of four types of CD4 effector T cells. We find that Erk2 is central to the contingencies governing the differentiation of Th1 cells and iTregs, and this is reflected in its effects on the subset-characteristic programs of gene expression. In particular, we show that a loss of *Erk2* caused a large-scale increase in gene expression, specifically under conditions of TGF-β signaling.

Materials and Methods

Mice and viral infection

CreER^{T2}, *Erk1*$^{-/-}$, *Erk2*$^{f/f}$ allele mice were described previously (8, 14, 15). Deletion of *loxP*-flanked alleles in *Erk2*$^{f/f}$ *CreER*^{T2} mice was induced by i.p. injection of 2 mg tamoxifen every day (Sigma) for six consecutive days, and mice were analyzed 2 d later. Where indicated, mice were infected i.p. with 2×10^5 PFU lymphocytic choriomeningitis virus (LCMV Armstrong). Bone marrow chimeras were made by reconstitution of lethally irradiated (10 Gy) *Rag1*$^{-/-}$ mice with T cell-depleted bone marrow cells from wild-type (WT; CD45.1$^+$) or *Erk2*$^{f/f}$ *CreER*^{T2} (CD45.2$^+$) mice separately or mixed at a 1:1 ratio. Mice were analyzed 8 wk after reconstitution. For Treg induction, *Erk2*$^{f/f}$ *CreER*^{T2} mice were crossed with Smarta transgenic mice (TCR transgenes specific for H2A^b bound with LCMV glycopeptide 61–80) (16). Animal work was performed according to University of California, San Diego (UCSD) guidelines.

Cell culture

CD4 T cells (purity > 90%) from lymph nodes and spleens were MACS purified (Miltenyi Biotec) by either positive selection for CD4 or by depletion using biotin-labeled B220, CD8, CD25, CD69, DX5, and MHC class II with streptavidin microbeads. T cell proliferation was stimulated with plate-bound anti-CD3 (5 ng/ml), with or without anti-CD28 added to the culture (1 μg/ml), as described (17). Where indicated, IL-2 (10 U/ml), PMA (20 ng/ml), and ionomycin (100 ng/ml) were added. For T cell differentiation, cells were stimulated with anti-CD3 and anti-CD28 plus IL-12 (10 ng/ml), IL-2 (50 U/ml), and anti–IL-4 (for Th1); IL-4 (10 ng/ml), IL-2, and anti–IFN-γ (for Th2); and IL-6, TGF-β, anti–IFN-γ, and anti–IL-4 (for Th17). To generate iTregs, CD4 cells were stimulated with anti-CD3, anti-CD28, TGF-β, and IL-2 (10 U/ml) in the presence or absence of anti–IL-4 and anti–IFN-γ. Cytokines were measured in the supernatant by ELISA (eBioscience).

Flow cytometry

Lymphocytes were explanted and stained with Abs specific for CD62L, CD44, CD4, and CD8. For the intracellular staining of Foxp3, cells were fixed and permeabilized with a Foxp3 buffer set (eBioscience). For Erk2 or phospho-Smad2,3 staining, cells were fixed with 2% p-formaldehyde and permeabilized with Perm III buffer (BD Biosciences). Cells were stained with Erk2- (Santa Cruz) or phospho-Smad2,3-specific Abs (Cell Signaling Technology), followed by goat anti-rabbit IgG-PE (Southern Biotech). For intracellular cytokines, cells were fixed and permeabilized with the BD Cytofix/Cytoperm Solution Kit (BD Biosciences) and stained for IFN-γ, IL-4, or IL-17 (eBiosciences). H2-A^b tetramers loaded with LCMV gp66–77 or human CLIP peptide 103–117 were provided by the National Institutes of Health tetramer facility. Samples were collected on a FACSCalibur or LSRII (BD Biosciences) and analyzed by FlowJo software (Tree Star). For CFSE analysis, cultures were resuspended in equal volumes and analyzed for a constant period of time. The numbers on the ordinate of graphs indicate the number of T cells per interval of intensity, where the area under the curve equals the total number of T cells collected.

Treg assays

In vitro Tregs were assayed as previously described (18). To generate $Foxp3^+$ T cells in vivo, 2×10^6 naive Smarta CD4 T cells ($CD45.2^+$) were transferred into B6 mice ($CD45.1^+$). The next day, recipient mice were immunized with 10 μg glycoprotein peptide (gp61–80) or sterile PBS. Five days later, spleens were harvested and analyzed for Foxp3 expression by flow cytometry.

Inflammatory bowel disease

Naive CD4 T cells ($CD25^-CD45RB^{hi}$) and Tregs ($CD25^+CD45RB^{low}$) were sorted on a FACSAria (BD Biosciences). Naive T cells (3×10^5) were transferred into $Rag1^{-/-}$ mice alone or together with 2×10^5 WT or $Erk2^{-/-}$ Tregs (19). Mice were weighed weekly and euthanized if their body weight decreased by >20%.

SDS-PAGE and Western blotting

SDS-PAGE and Western blotting were carried out as described (18). The following primary Abs were used: anti-Erk1, 2 (Santa Cruz), anti–phospho-Smad2, anti–phospho-Rsk3, anti–phospho-Mnk1 (Cell Signaling Technology), anti-ZAP70 (BD Biosciences), and anti-Bim (Sigma-Aldrich).

RNA isolation and quantitative real-time PCR

PCR and quantitative real-time PCR (qPCR) were carried out as described (18). Samples were normalized to *Gapdh* or *Ppia* (cyclophilin A). Primers used are available upon request.

Microarray analysis

Total RNA from WT and Erk2-deficient CD4 T cells were purified with an RNeasy kit (QIAGEN). Samples were processed by the Biomedical Genomics core, UCSD, using a MouseRef-8 BeadChip kit (Illumina). Interchip data were normalized by UCSD microarray core and further analyzed with Excel, GenePattern software suite (20), and TM4 microarray software suite (21). The sequences presented in this article have been submitted to Gene Expression Omnibus (http://www.ncbi.nlm.nih.gov/geo/) under accession number GSE37554.

Statistics

Prism 4.0c software (GraphPad software; San Diego, CA) was used for Student *t* test analyses. The *p* values are indicated in the figure legends.

Results

Erk2-deficient CD4 T cells from $Erk2^{f/f}$ $CreER^{T2}$ *mice*

We previously analyzed the effects of *Erk2* deletion on the function of $CD8^+$ T cells using a distal Lck promoter-Cre transgene (dLck-Cre); however, this transgene caused deletion in only 80% of CD4 T cells (22). To analyze the role of Erk2 signaling in peripheral CD4 T cells, we crossed $Erk2^{f/f}$ mice to $CreER^{T2}$ mice, and deletion of the *loxP*-flanked exons of *Erk2* was induced by tamoxifen (Fig. 1A) (15). By PCR, Western blot, and flow cytometry, the deletion of *Erk2* was uniform within the population and virtually complete. Tamoxifen-treated $Erk2^{f/f}$ $CreER^{T2}$ mice are referred to as $Erk2^{-/-}$. *Erk2* deletion led to reduced thymic cellularity, preferentially affecting the $CD4^+CD8^+$ population (8); however, $Erk2^{-/-}$ mice displayed similar proportions and numbers of CD4 and CD8 T cells within the secondary lymphoid tissues (Supplemental Fig. 1A). Similarly, naive and effector/memory cell populations based on CD44 and CD62L expression were also unchanged (Supplemental Fig. 1B).

Costimulation can replace the requirement for Erk2 in T cell proliferation

Consistent with our analysis of CD8 T cells (22), $Erk2^{-/-}$ CD4 T cells, stimulated with anti-CD3 in the absence of added costimulation, accumulated at the undivided stage (Fig. 1B) and displayed incomplete induction of CD25 and CD44 (Fig. 1C). Higher concentrations of anti-CD3 did not induce proliferation (data not shown). However, the defect in $Erk2^{-/-}$ CD4 T cell proliferation was rescued by the addition of a CD28-mediated costimulatory signal (Fig. 1B, 1C). In fact, $Erk2^{-/-}$ T cells appeared to undergo more rounds of division compared with WT T cells; one explanation is suggested by the Erk2 dependence of the cyclin-dependent kinase inhibitor, $p21^{Cip1/Waf1}$, as shown below. Contrary to our expectations, similar results were obtained using T cells deleted for both *Erk1* and *Erk2* (data not shown). These results imply that a signaling pathway downstream of the costimulatory receptor CD28 can replace a requirement for Erk activation in TCR-mediated cell cycle progression.

Similar to CD8 T cells, proliferation and survival were only partially rescued by the addition of IL-2 (Supplemental Fig. 1C) (22). However, $Erk2^{-/-}$ CD4 T cells proliferated to the same extent as did WT T cells upon PMA and ionomycin stimulation (Supplemental Fig. 1D). Finally, in marked contrast to the results with $Erk2^{-/-}$ T cells, there was no effect of *Erk1* deletion on $CD4^+$ T cell proliferation in response to TCR-mediated stimulation, with or without costimulation (Supplemental Fig. 2A).

Erk2 is required for Th1, but not for Th2 or Th17, development in vitro

Because T cells can proliferate in the absence of Erk2, we were able to examine the role of Erk1 or Erk2 in Th1, Th2, or Th17 differentiation. There were no differences observed for WT and $Erk1^{-/-}$ cells when activated under the different Th (Th1, Th2, Th17) conditions (Supplemental Fig. 2B–D) (23). In contrast, $Erk2^{-/-}$ CD4 T cells displayed normal proliferation but a survival defect when activated under Th1- and Th2-polarization conditions (Fig. 2A). This survival defect may be the result of increased levels of the proapoptotic protein Bim that were observed in $Erk2^{-/-}$ cells relative to WT cells (Fig. 2B).

We further examined whether the loss of Erk2 affected the differentiation of Th1, Th2, and Th17 cells, as measured by the intracellular production of IFN-γ, IL-4, or IL-17 (Fig. 2C). The proportion of IFN-γ–producing Erk2-deficient CD4 T cells and the amount of IFN-γ/cell were reduced compared with WT cells, and there was a 4-fold decrease in IFN-γ levels measured in the

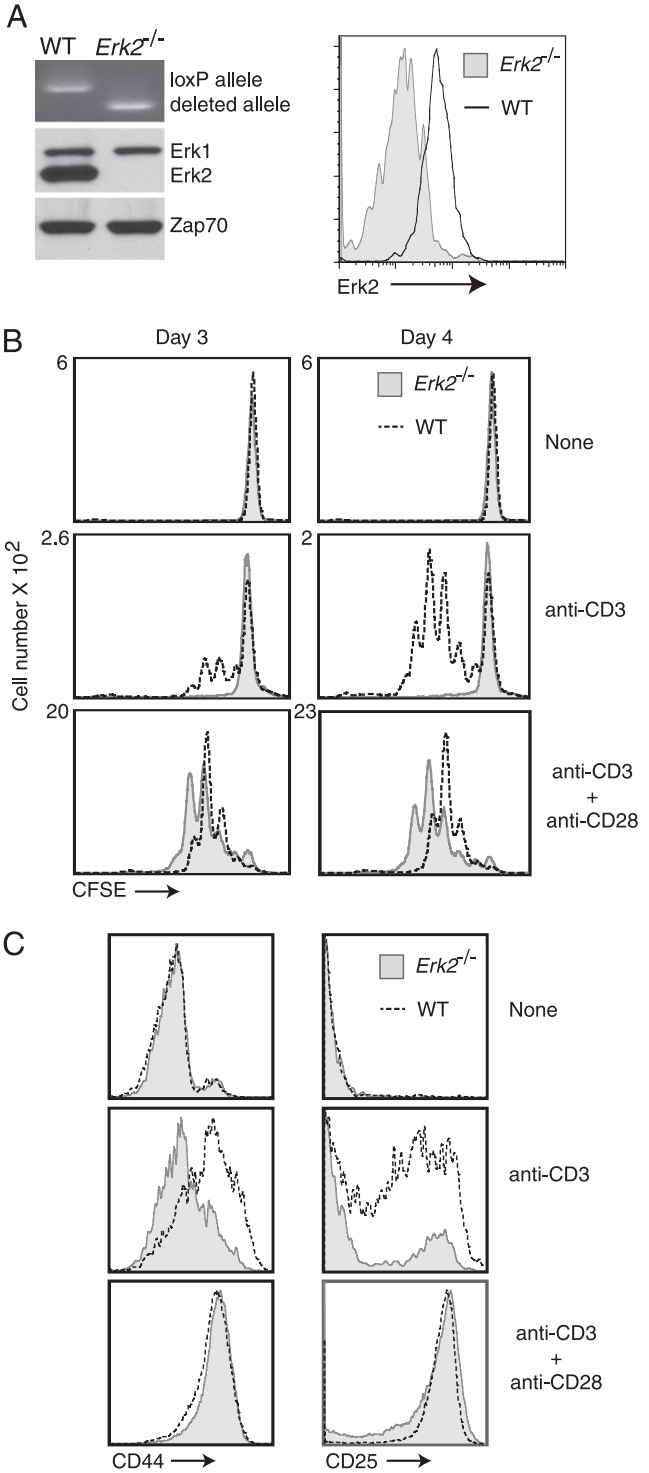

FIGURE 1. *Erk2*$^{-/-}$ T cells require costimulation for cell cycle progression. (**A**) Purified CD4 T cells from lymph nodes and spleen were analyzed for the presence of Erk2 by PCR, Western blotting, and flow cytometry. (**B**) Purified WT or *Erk2*$^{-/-}$ CD4 T cells were stimulated in vitro. CFSE profiles were analyzed for CD4$^+$ T cells. (**C**) T cells (WT, *Erk2*$^{-/-}$) were analyzed for CD25 and CD44 expression on day 3 following the stimulation. Similar results were found on day 4. The data are representative of three or more independent experiments.

culture supernatant (Fig. 2D). Despite this defect, T-bet and p-Stat1 were induced in *Erk2*$^{-/-}$ T cells to an extent equivalent to WT T cells (Fig. 2G). In addition, under Th1 conditions, *Erk2*$^{-/-}$ CD4 T cells exhibited higher Gata-3 expression, consistent with increased IL-4–independent Th2 differentiation found under conditions of Erk attenuation (10, 11). In contrast, the amount of p-Stat5 was reduced (Fig. 2G). Under optimal, polarizing Th2 conditions, there was a trend toward increased Th2 differentiation, but the difference did not reach significance given the number of trials (Fig. 2C, 2E). There was no difference in Th17 differentiation in the absence of Erk2 (Fig. 2C, 2F).

Impaired Th1-driven viral response in Erk2-deficient mice

To examine differentiation of Th1 cells in vivo, we infected WT, *Erk1*$^{-/-}$, or *Erk2*$^{-/-}$ mice with LCMV Armstrong and assessed the number of IFN-γ–producing T cells at day 8 postinfection. *Erk1*$^{-/-}$ and WT mice displayed similar CD4 responses, whereas there was a substantial reduction in the proportion and the absolute cell number of IFN-γ–producing cells in *Erk2*$^{-/-}$ mice (data not shown). To determine whether this effect was T cell intrinsic, *Rag1*$^{-/-}$ mice were reconstituted with bone marrow cells from WT or *Erk2*$^{f/f}$ *CreER*^{T2} mice or an equal mixture of both. Eight weeks postreconstitution, the mice were treated with tamoxifen and challenged with LCMV. The number of Ag-specific CD4 T cells, as measured by MHC class II gp66–77 tetramers or antiviral IFN-γ–producing Th1 cells, was dramatically reduced in the mice that were reconstituted with *Erk2*$^{f/f}$ *CreER*^{T2} cells (Fig. 3). Even within the mixed bone marrow chimeras, the population of Ag-specific *Erk2*$^{-/-}$ T cells was reduced compared with WT T cells in the same animals. The number of tetramer$^+$ cells was approximately equivalent to the number of IFN-γ$^+$ T cells; thus, the absence of Erk2 did not redirect differentiation, but it either diminished Th1 differentiation or survival.

Increased iTreg differentiation in absence of Erk2

The role of Erk in the differentiation of iTregs in culture was examined. *Erk2*$^{-/-}$, but not *Erk1*$^{-/-}$, T cells generated increased proportions and numbers of CD25$^+$Foxp3$^+$ iTregs (Fig. 4A, 4B, data not shown). iTregs were also induced in vivo by transferring naive Smarta CD4 T cells (depleted of CD4$^+$CD25$^+$ cells) and immunizing mice with LCMV gp61–80. Under these conditions, there was an increased proportion of *Erk2*$^{-/-}$ Smarta T cells that converted to Foxp3$^+$ cells (Fig. 4C). In addition, there was an increase in the proportion of Foxp3$^+$ natural Tregs present in lymphoid organs of *Erk2*$^{f/f}$ *Cd4Cre* mice (data not shown).

To determine whether *Erk2*$^{-/-}$ Tregs were functional, we used cell culture and in vivo measures of Treg activity. As shown, CD4$^+$ CD25$^+$ cells from *Erk2*$^{-/-}$ mice were at least as effective as WT Tregs in their ability to inhibit T cell proliferation (Fig. 4D). *Erk2*$^{-/-}$ Tregs also suppressed weight loss in an inflammatory bowel disease model to the same extent as did WT Tregs (Fig. 4E) (24). We can conclude that *Erk2*$^{-/-}$ T cells more readily differentiate into iTregs, and *Erk2*$^{-/-}$ natural Tregs exhibit at least equivalent function compared with those from WT mice.

Erk2 dependence of Dnmt *expression and Smad signaling*

The regulation of *Foxp3* depends importantly on methylation, such that, in the absence of Dnmt1, *Foxp3* is efficiently expressed in activated CD4 and CD8 T cells (25–27). Thus, we considered the possibility that enhanced iTreg induction in *Erk2*$^{-/-}$ T cells was the result of reduced *Dnmt1* expression. Analysis by qPCR indicated that *Dnmt1* expression is progressively induced with time, and the induction is partially Erk2 dependent (Fig. 5A) at 2 d in culture. As shown below, *Foxp3* is induced by 1 d, and its expression is enhanced in *Erk2*$^{-/-}$ cells. Thus, simple regulation of *Dnmt1* mRNA does not appear to explain the TGF-β–induced Foxp3 induction.

Another potential mode of regulation is direct inhibition of TGF-β signaling through the inhibitory phosphorylation of Smad2

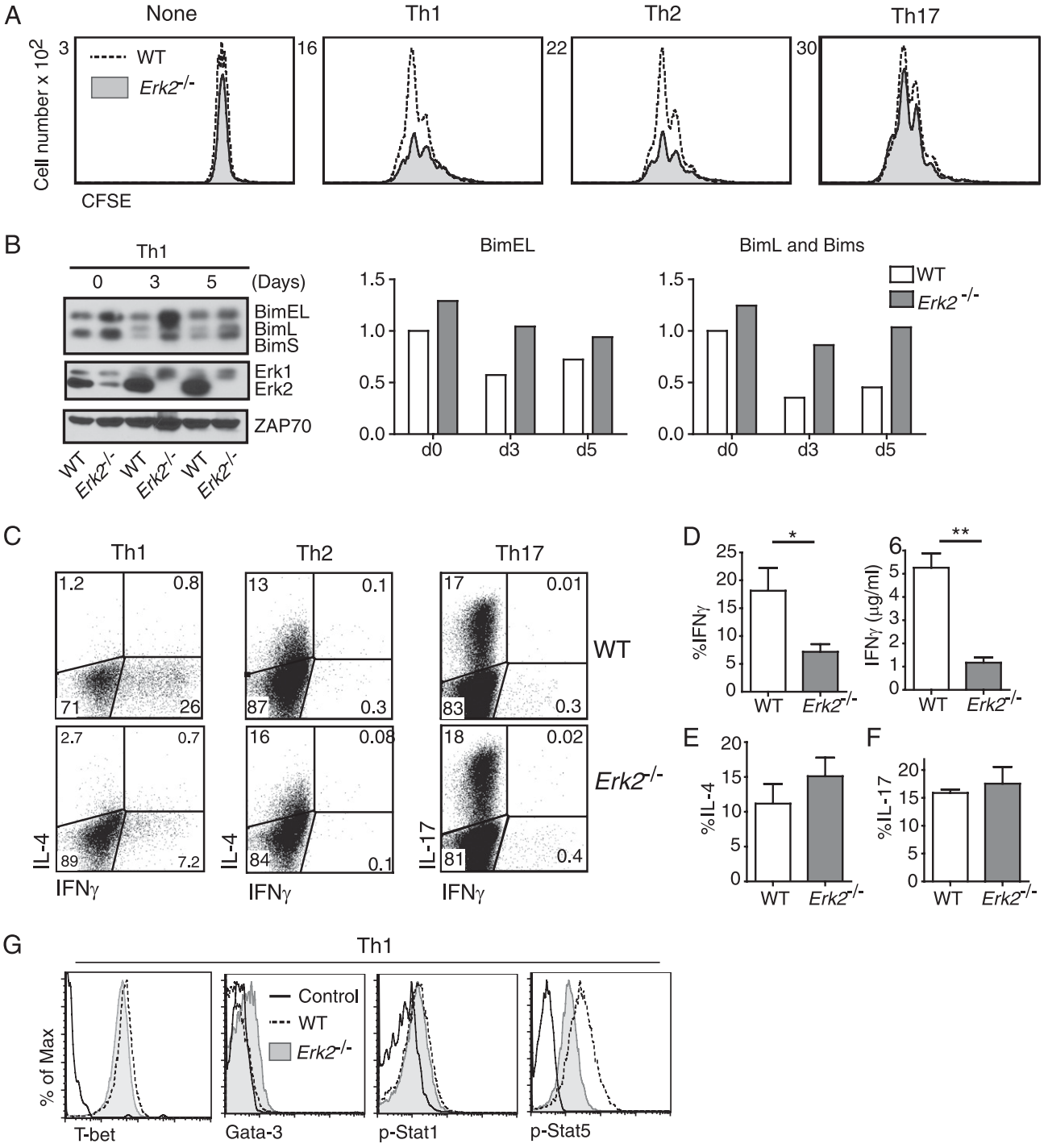

FIGURE 2. *Erk2*$^{-/-}$ CD4 T cells display impaired survival and polarization to the Th1 subset. (**A**) CD4 T cells were cultured under different conditions for 3 d. CFSE profiles were analyzed as in Fig. 1 (representative of three experiments). (**B**) Purified CD4 T cells from WT and *Erk2*$^{-/-}$ mice were cultured for Th1 polarization. Cell lysates were analyzed by Western blotting, and the amounts of BimEL and BimL/S were normalized to ZAP70 (representative of three separate experiments). (**C**) Cells were cultured in polarizing conditions, and CD4$^+$ T cells are shown (representative of three experiments). (**D**) The percentage of IFN-γ$^+$ T cells and the amount of IFN-γ from cultures of restimulated Th1 cells (mean ± SEM from three experiments). Percentages of IL-4–producing (**E**) and IL-17–producing (**F**) cells (mean ± SEM from three experiments). (**G**) T cells were analyzed for T-bet, Gata-3, p-Stat1, and p-Stat5 at day 3. Isotype (mouse IgG1) control was used for T-bet and Gata-3 staining; goat anti-rabbit PE was used for the p-Stat–staining control. Representative of three experiments. *$p < 0.05$, **$p < 0.001$.

and Smad3 at their linker regions, as shown by the analysis of Mekk2,3-deficient T cells (28). Because Mekk2,3 are upstream of all of the MAPKs, the possibility exists that Erk constitutes the primary mediator of this effect. Smads are activated by TGF-βRI–mediated phosphorylation at the C-terminal SXS motif; this, in turn, causes nuclear localization and downstream gene activation. As a means of detecting activated Smad2 and Smad3, we probed the amount of SXS phosphorylation of Smad2/3 both by intracellular fluorescence staining and immunoblotting. The results showed an increased induction of pSmad2 in Erk2-deficient cells compared with WT cells by 30 min, and this difference was enhanced at 2–3 d after stimulation (Fig. 5B, 5C). We conclude that

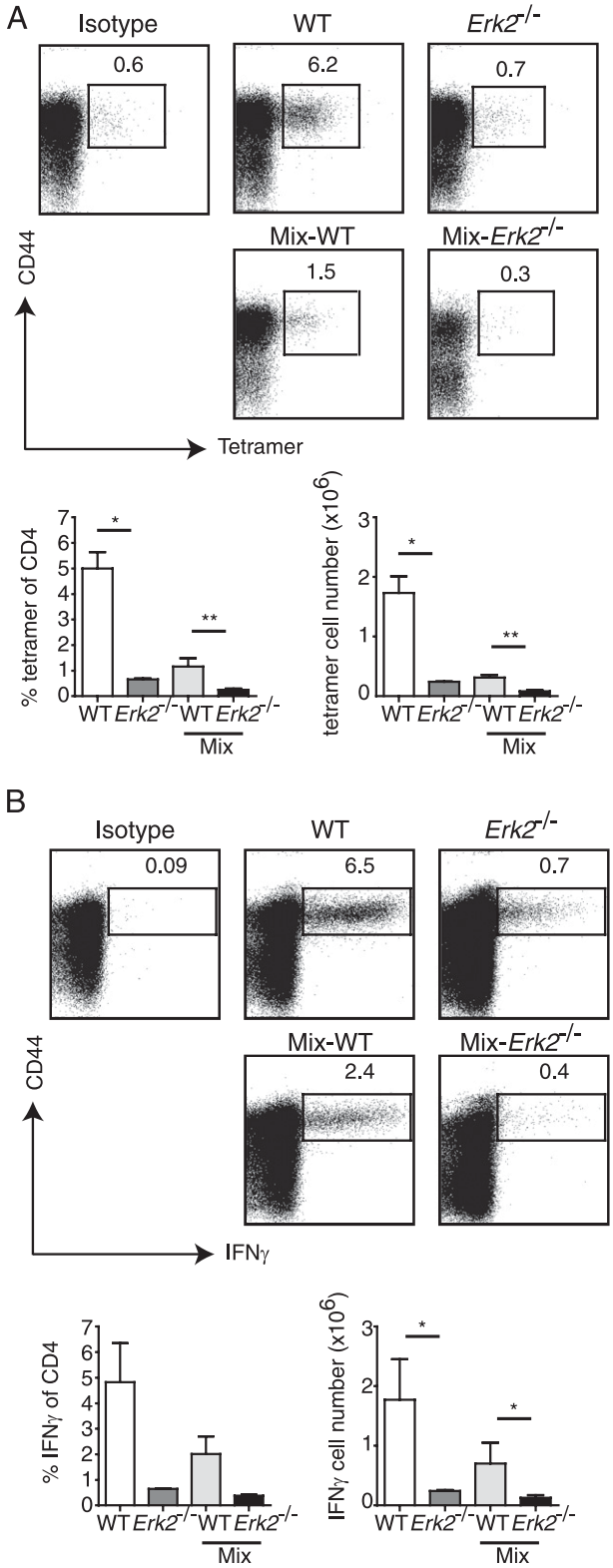

FIGURE 3. Impaired antiviral Th1 responses in the absence of Erk2. (**A** and **B**) Single or mixed bone marrow chimeras were treated with tamoxifen for 6 d, rested for 2 d, and then infected with LCMV. (A) $CD4^+$ T cells were analyzed by staining for CD44 and $H2A^b$ tetramer bound with gp66–77 or CLIP peptide (control). (B) $CD4^+$ T cells were stained for CD44 and intracellular IFN-γ following restimulation with the LCMV peptides gp61–80 and NP309–327. Data are mean ± SEM of Ag-specific CD4 T cells (n = 3/group) present in spleen for a single experiment. Data shown are representative of three independent experiments carried out on three different sets of mice. *$p < 0.05$, **$p < 0.001$.

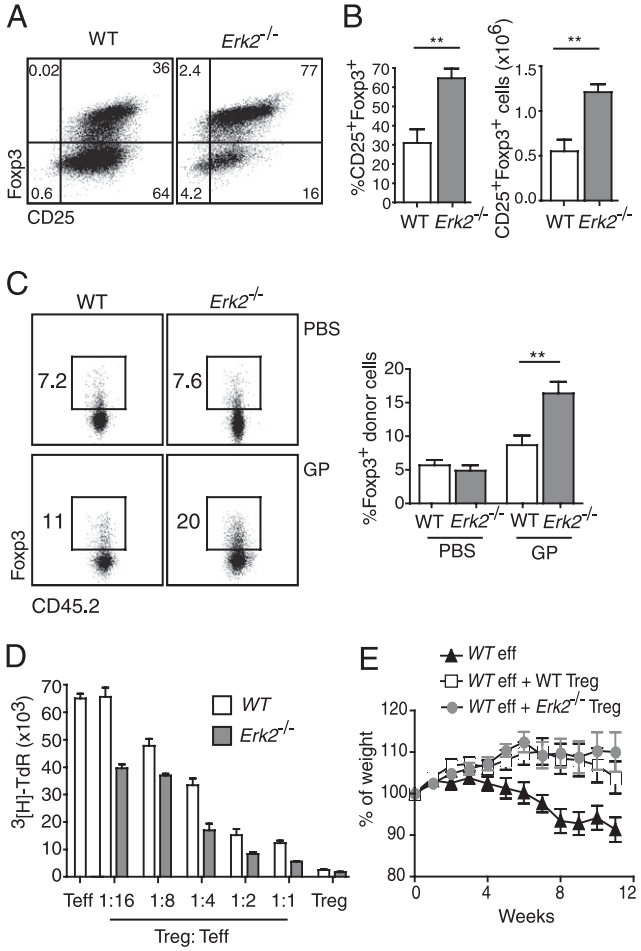

FIGURE 4. Enhanced differentiation and normal function of induced Tregs in the absence of Erk2. (**A** and **B**) Purified CD4 T cells were stimulated under iTreg conditions for 5 d and analyzed for CD4, CD25, and Foxp3 expression. (A) Representative profiles. (B) Accumulated results from all four experiments (mean ± SEM). (**C**) Induction of Smarta transgenic iTregs in vivo. Representative flow cytometry profiles (gated on $CD4^+$ and $CD45.2^+$ cells) with the mean percentages of $Foxp3^+$ cells within the donor Smarta T cells graphed. Data were accumulated from two independent experiments (PBS, n = 8; gp peptide, n = 10). (**D**) WT effector T cells ($CD4^+CD25^-$) were cocultured with WT or $Erk2^{-/-}$ Tregs ($CD4^+CD25^+$), and proliferation was measured by the incorporation of [^{3}H]deoxythymidine (TdR). The data are representative of three independent experiments. (**E**) Weight loss associated with inflammatory bowel disease. Data are from three independent experiments (total mice: WT eff, n = 14; WT eff + WT Treg, n = 11; WT eff + $Erk2^{-/-}$ Treg, n = 9). **$p <$ 0.001.

inactivation or removal of Erk2 promotes greater Smad signaling, which, in turn, enhances Treg development.

iTreg gene expression is suppressed by Erk2

To further understand the role of Erk2 in T cell differentiation, we performed microarray analyses of WT and $Erk2^{-/-}$ T cells in eight conditions. Basic analyses revealed that the data set reflects Erk2-dependent, T cell-specific mRNA expression under multiple stimulatory and polarizing conditions (Supplemental Fig. 3A). To identify a set of genes dependent on Erk2 for expression, we averaged the ratios (WT/$Erk2^{-/-}$) across all eight conditions. There were 49 Erk2-dependent probes (mean ratio > 1.5), and the highest 14 are shown as a correlated heat map (Supplemental Fig. 3B). These include 3/3 *Mapk1* (*Erk2*); 2/2 *Dusp6*, an Erk dual-

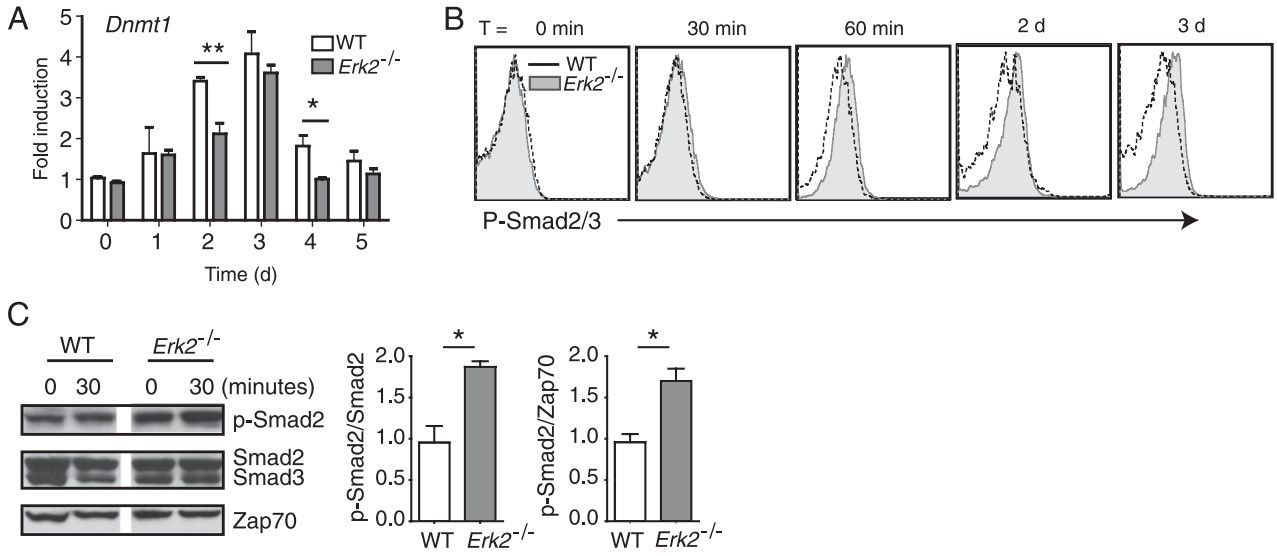

FIGURE 5. Erk2 regulates DNMT and phosphorylation of Smad2. (**A**) WT or *Erk2*$^{-/-}$ cells from individual mice were stimulated under iTreg conditions for 0–5 d. The mRNA samples were analyzed by real-time quantitative PCR for *Dnmt1* in duplicate and normalized to the *Ppia* gene (± SEM) (WT, $n = 3$; *Erk2*$^{-/-}$, $n = 3$). The data are representative of two separate experiments. (**B**) WT or *Erk2*$^{-/-}$ naive CD4 T cells were stimulated under iTreg conditions and analyzed for pSmad2,3 expression by flow cytometry (representative of three experiments). (**C**) Purified CD4 T cells from WT and *Erk2*$^{-/-}$ mice were stimulated under iTreg conditions for 30 min. Cell lysates were analyzed by Western blotting at the indicated time points. ZAP70 was used as loading control. Plots show the phospho-Smad2 density normalized to Smad2 or ZAP70. Relative expression level was normalized by WT day 0 expression, as 1. The data plotted in the bar graphs were accumulated from three independent experiments. $*p < 0.05$, $**p < 0.01$.

specific phosphatase (29); *Egr2*, a direct Erk target; *Ccl1*, encoding a ligand of Ccr8; *Gpr68*, a G-coupled proton sensor; and *Tnf*. We note the alternating pattern of Erk2 dependence. In contrast, only 10 probes were suppressed by Erk2 (mean ratio < 0.67) (Supplemental Fig. 3C). These include *Ccr8*; *Ebi2*, an oxysterol-specific nuclear receptor controlling T and B cell migration (30); *Gata3*; and *Klf2*, a Foxo1 target controlling T cell homing (31). We conclude from these analyses that the data set reflects Erk2-dependent T cell-specific mRNA expression under multiple stimulatory conditions.

Scatter plots comparing *Erk2*$^{-/-}$ with WT values under 1-d Th0 or Th1 conditions identified a small number of probes for which *Erk2*$^{-/-}$ was >1.5 or <0.67 compared with WT: 71 probes (45 suppressed by Erk2, 26 dependent on Erk2) for Th0 and 77 probes (42 suppressed by Erk2, 35 dependent on Erk2) for Th1. In contrast, the same comparison under 1-d iTreg conditions identified 643 probes, a >8-fold increase over the number identified under Th0 or Th1 conditions (544 suppressed by Erk2, 99 dependent on Erk2) (Fig. 6A). Using Venn diagrams, we graphed the number of overlapping or unique probes that were suppressed by or dependent on Erk2 under each of the polarizing conditions. The Erk2-suppressed changes in gene expression specific to iTregs (503 probes) constituted, by far, the largest category (Fig. 6B).

This large-scale increase in gene expression at 1 d in *Erk2*$^{-/-}$ T cells could be consistent with a hypomethylated genome as a result of reduced *Dnmt1*; however, the qPCR data showed no Erk2-dependent difference in *Dnmt1* expression at this time point (Fig. 5A). The array data showed that, of the *Dnmt* isoforms assessed, only *Dnmt1* and *Dnmt3b* were expressed over background, and neither was affected by the addition of TGF-β (Fig. 6C): equivalent induction was seen at 1 d under Th0, Th1, and iTreg conditions of stimulation. Moreover, the effects of *Erk2* deletion on *Dnmt1* and *Dnmt3b* expression were small compared with the magnitude of induction. We conclude that Erk2 signaling constitutes an important suppressor of gene expression in the presence of TGF-β, although the extent to which this results from *Dnmt1* regulation is unknown (discussed below).

Thus, the iTreg dependence on Erk2 provided a tool to more finely characterize a program of iTreg-specific genes. We identified those genes that were induced in 1-d iTreg conditions, but not under Th0 or Th1 conditions, and were suppressed by Erk2 (Fig. 6D). This algorithm identified 45 unique probes, including all 3 probes specific for *Foxp3* and both probes specific for the Treg-specific neuropilin-1 (*Nrp1*). *Gpr83*, *Ecm1*, *Cmtm7*, *Nkg7*, *Socs2*, and *Glrx* were previously found to be iTreg specific (32); of these, we also identified *Gpr83* and *Nkg7*. *Socs2* was strongly (>10-fold) induced in Th0, Th1, and iTreg conditions (see below) and, thus, was not iTreg specific (Fig. 7D). *Ecm1* was induced at 3 h but not at 1 d. *Cmtm7* and *Glrx* were relatively unchanged across all conditions (data not shown).

Other genes identified in this subset that may be involved in immune function included *Dscr1l2*, which inhibits calcineurin-dependent transcriptional responses; *Ctsw* (cathepsin W), which functions in T cell cytolytic activity; *Faim3*, a caspase-8 inhibitor; *Rcan3*, which binds and inhibits calcineurin A; *Tnfrsf1b* (TnfRII); and *Tnfrsf9* (4-1BB) (Fig. 6D). We also analyzed gene expression at 3 h postactivation, with or without the addition of TGF-β. The rationale was that gene expression directly affected by TGF-β signaling would be induced early, yet none of the probes specific to iTreg induction at 1 d were already induced at 3 h in the presence of TGF-β. All of the probes induced at 3 h with TGF-β were also induced in its absence under Th0 conditions (Fig. 6D). Likewise, we examined whether stimulation with TGF-β for 1 or 3 h after 1 d of Th0 activation would induce a subset of the signature genes, and we identified five of the genes listed in Fig. 6D. These included *Ccr8*, *Ctsw*, *Dscr1l2*, *Emp1*, and *Edod1*. *Foxp3* and *Nrp1* were not induced under these conditions. We conclude that the iTreg program of gene expression becomes elaborated in naive T cells between 3 h and 1 d post–TGF-β stimulation.

A separate analysis of the array data based on an unbiased hierarchical clustering of the entire data set (Pearson correlation, average linkage) was carried out, and a heat map of a cluster containing *Foxp3* was selected (Supplemental Fig. 4A). Although there is a large overlap in the genes identified using the algorithm

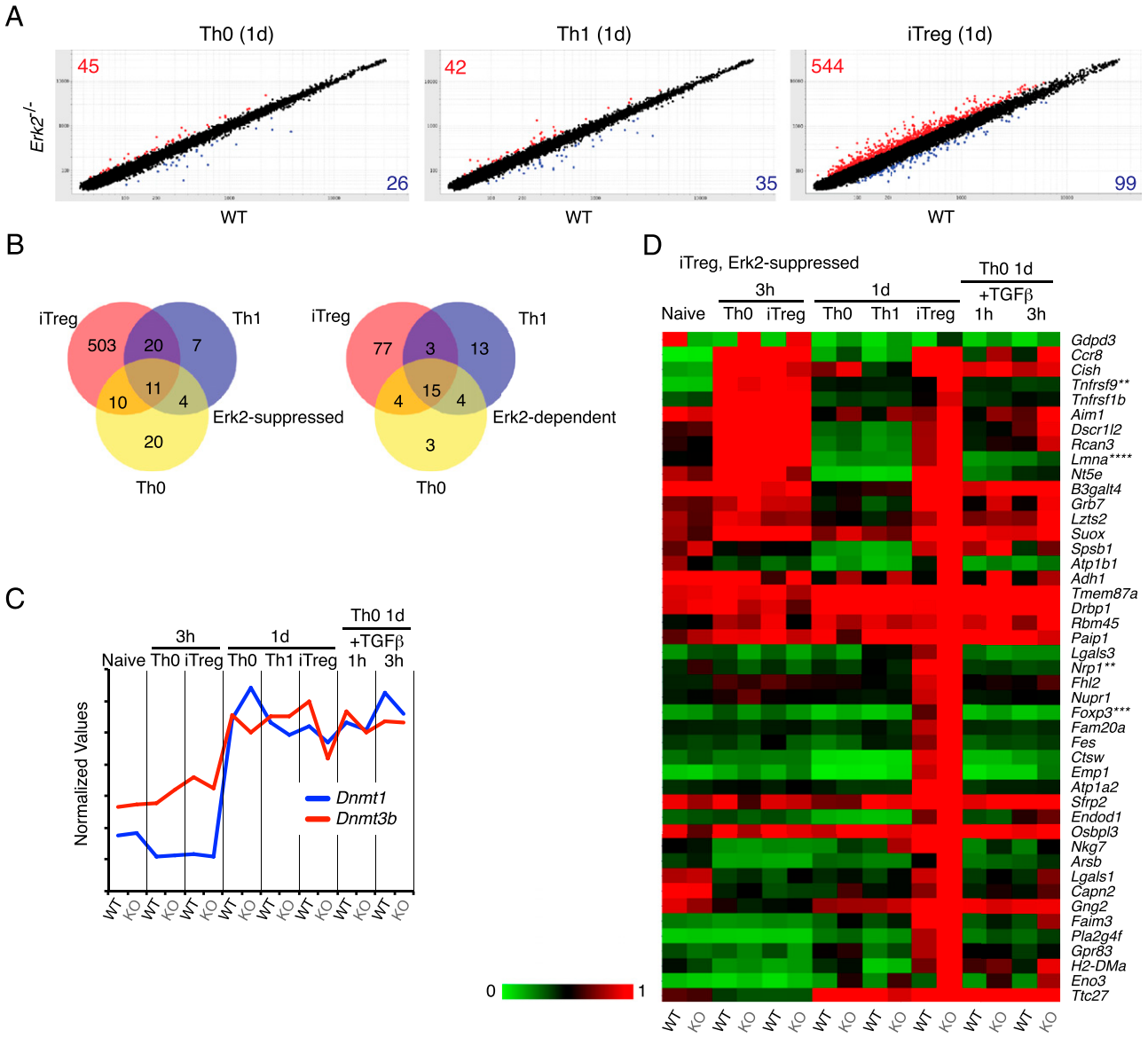

FIGURE 6. Microarray analysis of gene expression in WT and *Erk2*$^{-/-}$ CD4 T cells. (**A**–**D**) RNA samples were isolated from WT or *Erk2*$^{-/-}$ (KO) T cells that were cultured as follows: naive (0 d); Th0 (CD3, CD28, IL-2) 3 h; iTreg (Th0, TGF-β) 3 h; Th0 1 d; Th1 (Th0+IL-12+anti–IL-4) 1 d; iTreg 1 d; Th0 1d + TGF-β 1 h; Th0 1d + TGF-β 3 h. (A) The values for *Erk2*$^{-/-}$ versus WT for each probe are presented as scatter plots for Th0, Th1, and iTreg conditions at 1 d. Numbers indicate genes with a difference in expression >1.5-fold (Erk2 suppressed; top left, red dots) or <0.67-fold (Erk2 dependent; bottom right, blue dots). (B) The numbers of Erk2-dependent or Erk2-suppressed genes from the scatter analysis (A) are shown in Venn diagrams to indicate the overlap between each category. (C) The values of probes for *Dnmt1* and *Dnmt3b* were normalized to the median for each probe and charted for all eight conditions indicated on the figure alternating between WT and KO. (D) The Erk2-suppressed iTreg genes were identified, and the expression values were normalized to the maximum for each probe, ordered by hierarchical clustering (Pearson correlation) and depicted as a correlated heat map. The criteria were iTreg inducible, iTreg 1 d *Erk2*$^{-/-}$ > (1.5) 0 d *Erk2*$^{-/-}$; TGF-β dependent, iTreg 1 d *Erk2*$^{-/-}$ > (1.5) Th0 1 d *Erk2*$^{-/-}$; not Th1, iTreg 1 d *Erk2*$^{-/-}$ > (1.5) Th1 1 d *Erk2*$^{-/-}$; and Erk2 suppressed, iTreg 1 d *Erk2*$^{-/-}$ > (1.3) iTreg 1 d WT. The criteria were chosen for biological relevance and to identify a manageable set of genes. Asterisks indicate the number of probes identified for each gene if >1.

described above (e.g., *Nrp1*), unique genes were also identified. Notably, this list includes *Ccr6*, encoding a chemokine receptor that plays a role in inflammatory bowel disease (33), and three transcription factors not previously known to play a role in Treg differentiation: *Cux1*, *Stat5*, and *Zfhx3* (discussed below).

Gene expression associated with Th0, Th1, and Th2 polarization

For each of the T cell subsets (Th1, Th2, Th17, and iTreg), there is a transcription factor, which, if not a lineage-specification factor, is characteristic and essential for function. As such, we charted the profiles of *T-bet* (*Tbx21*), *Gata3*, *Rorγ* (*Rorc*), and *Foxp3* (Fig. 7A, Supplemental Fig. 4B) over the conditions tested. Remarkably, the profiles for *Tbx21* (*T-bet*) and *Gata3* were mirror images of one another, both for conditions of induction and Erk2 dependence. For all eight conditions, *Tbx21* was dependent on Erk2, and Gata3 was suppressed by Erk2. This graphically illustrates the polarity of these two T cell subsets and reinforces the Erk2 dependence of Th1 differentiation contrasted with enhanced Gata-3 expression and Th2 differentiation found under conditions of Erk2 attenuation (Figs. 2C–G, 3A, 3B) (11). Equally striking was the profile of *Foxp3*. It was only induced under iTreg conditions for 1 d; consistent with increased induction of iTregs from Erk2-deficient precursors, its expression was further enhanced 2-fold by the de-

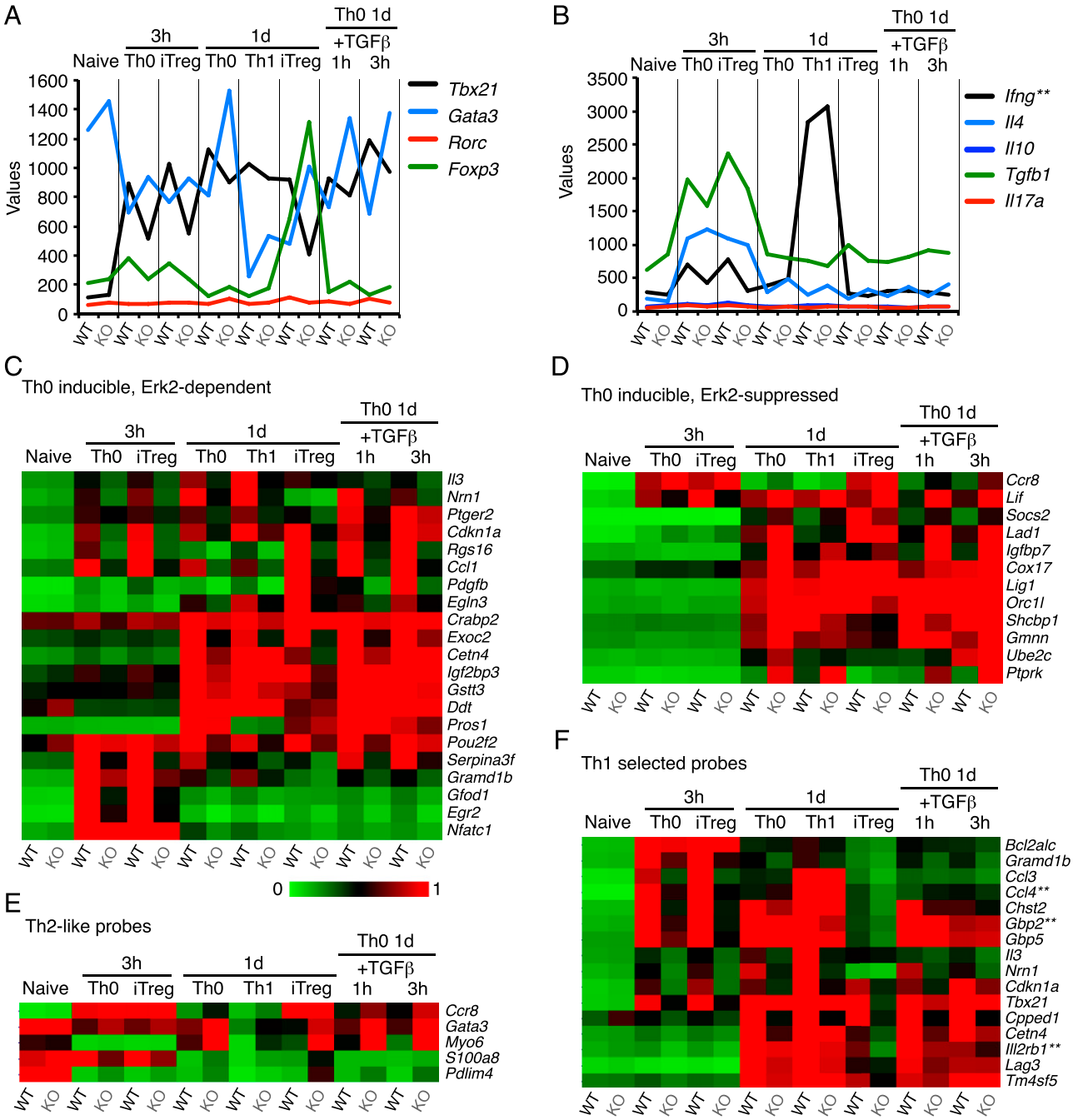

FIGURE 7. T cell subset array analyses. (**A**) The array values for *Tbx21*, *Gata3*, *Rorc*, and *Foxp3* were charted. See legend for Fig. 6. (**B**) The array values for the signature cytokines *Ifng*, *Il4*, *Il10*, *Tgfb1*, and *Il17a* were charted. (**C–E**) Correlated heat maps of subset genes were identified as described in the legend for Fig. 6. (C) Th0, Erk2-dependent probes: inducible, Th0 1d WT > (2) 0 d WT; Erk2-dependent, Th0 1 d WT > (1.5) Th0 $Erk2^{-/-}$ 1d. (D) Th0, Erk2-suppressed probes: inducible, Th0 1 d WT > (2) 0 d WT; Erk2-suppressed, Th0 1 d $Erk2^{-/-}$ > (1.3) Th0 1 d WT. (E) Th2-like probes: Erk2-suppressed, Th0 1 d $Erk2^{-/-}$ > (1.5) Th0 1 d WT; Not Th1, Th0 1d $Erk2^{-/-}$ > (3) Th1 1d WT. (**F**) Th1-selected probes: inducible, Th0 1 d WT > (3) 0 d WT and Th1 1 d WT > (3) 0 d WT; Th1 not iTreg, Th1 1 d WT > (2) iTreg 1 d $Erk2^{-/-}$; early-onset Erk2-dependent, Th0 3 h WT > (1.3) Th0 3 h $Erk2^{-/-}$.

letion of *Erk2* (Fig. 7A, Supplemental Fig. 4A). In addition, under iTreg conditions, *Erk2* deletion attenuated *Tbx21* and enhanced *Gata3*, gene expression predicted to further promote iTreg differentiation (34, 35). *Rorγ* (*Rorc*) expression was not detected.

This analysis was extended by an examination of the signature cytokines for the different T cell subsets (Fig. 7B). IFN-γ was only induced under Th1 conditions, but it was not appreciably dependent on Erk2. Because the mean fluorescence intensity of intracellular IFN-γ was higher in WT versus Erk2-deficient T cells (Fig. 2C), there may be a posttranscriptional Erk2-dependent enhancement. IL-4 was induced at 3 h under Th0 conditions, but it was close to baseline levels by 1 d. TGF-β, sometimes characteristic of iTregs, was induced at 3 h but not at 24 h, and IL-10 was not induced under any conditions. These data reveal that there is not a strict correlation between the lineage-characteristic transcription factors and subset-specific cytokines; this underscores the notion that T cell differentiation is not governed by the expression of a single, signature transcription factor (36, 37).

In addition, we analyzed those genes that are dependent on Erk2 and induced under different conditions of T cell activation. Twenty-one unique probes were induced under Th0 conditions at 1 d and were dependent on Erk2 (Fig. 7C). This set contained *Egr2*, *Ccl1*,

Cdkn1a (*p21*$^{Cip1/Waf1}$), and *Nfatc1*. Further analysis showed that *p21*$^{Cip1/Waf1}$ was the only cyclin-dependent kinase inhibitor that was dependent on Erk2 under any of the conditions tested (data not shown). It is essential for the prevention of excess numbers of T cells and the onset of a lupus-like autoimmune syndrome (38). Twelve Th0-inducible probes were suppressed by Erk2, including *Ccr8*, *Lif*, and *Socs2*, a positive regulator of cytokine signaling (Fig. 7D) (39).

We did not analyze gene expression under Th2 conditions, but we looked for genes whose expression was similar to the pattern of *Gata3* (i.e., *Erk2*$^{-/-}$ Th0 was greater than WT Th0, and *Erk2*$^{-/-}$ Th0 was much greater than WT Th1). This resulted in the identification of only five probes, including *Gata3* and *Ccr8*, a chemokine receptor required for the recruitment of Th2 cells to allergen-inflamed skin (40) (Fig. 7E). A similar analysis was carried out for Th1 signature genes, looking for probes that were dependent on *Erk2* and preferentially induced in Th1 cells compared with iTregs (Fig. 7F). We identified 16 genes, including *Ccl3*, *Ccl4*, *Cdkn1a* (*p21*$^{Cip1/Waf1}$), *IL12rb1* (IL-12R), and *Tbx21* (T-bet). We did not identify any additional transcription factors that were specific to the Th1 subset.

Erk2-dependent cell survival

Because there was a marked loss of T cell survival correlated with increased Bim expression in Erk2-deficient T cells under Th1 conditions (Fig. 2B), we plotted the Bcl-2 family members and found five that were highly regulated under the conditions tested (Fig. 8). *Bcl2* and *BclX*$_L$ (*Bcl2l1*) were mirror images with respect to T cell activation and Erk dependence, with *Bcl2* being weakly suppressed by *Erk2* and *BclX*$_L$ being weakly dependent on *Erk2*. Proapoptotic *Bim* was moderately suppressed by *Erk2*, consistent with the data presented in Fig. 2B and loss of survival under Th1 conditions. Interestingly, we found that the prosurvival genes *Bcl2a1c* and *Bcl2a1d* displayed expression patterns almost identical to that of *Bim*. The regulation of mitochondrial death in T cells in different phases of activation and differentiation is clearly complex.

Discussion

Depending on cytokines and costimulation, strong activation can favor a Th1 response, whereas weaker activation favors either a Th2 response or iTreg differentiation (36, 41). In this study, we show that this strength of signaling contingency is mediated, in part, through Erk2. Although we found no phenotypic effect of *Erk1* deletion, the effects of *Erk2* deletion mimicked a weak signal, inhibiting Th1 differentiation while promoting iTreg differentiation. In addition, gene-expression studies clearly illustrated the polarity of Th1 versus Th2 differentiation based on the presence or absence of Erk2. The origin of Erk1 and Erk2 differences is unknown, but their differential association with upstream kinase-signaling complexes or localization within the cell may provide important information with respect to the signaling important for T cell differentiation.

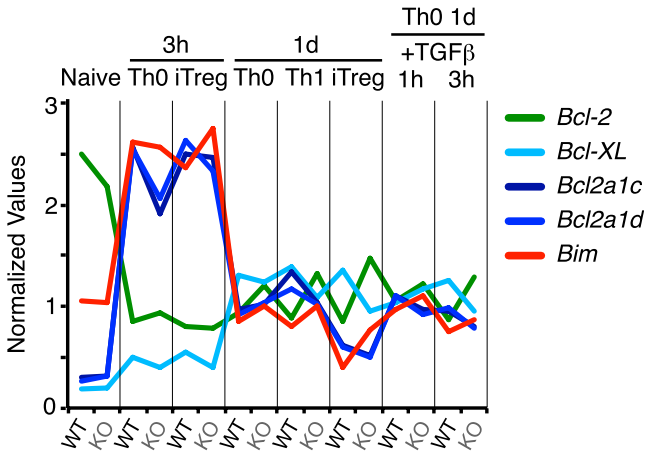

FIGURE 8. Expression of Bcl-2 family members. The median normalized array values for Bcl2, Bcl2l1 (BclxL), Bcl2a1c, Bcl2a1d, and Bim were charted.

Under conditions supporting Th1 differentiation both in culture and in response to LCMV infection, the loss of Erk2 resulted in a decreased accumulation and percentage of IFN-γ$^+$ cells. This is consistent with a study showing that impaired H-ras and K-ras resulted in decreased IFN-γ expression (42). Reduced Th1 survival in the absence of *Erk2* correlated with the increased expression of all three forms of Bim, including the highly apoptogenic Bim$_S$ form (43). From the array data, this is due, at least in part, to differences in RNA expression, as we showed for CD8 T cells (22). In addition, *Bcl-2* expression was reduced upon T cell activation, whereas *Bcl-X*$_L$ was increased (44), and these changes were dampened in the absence of Erk2. The *Bcl2a1* paralogs, like *Bim*, were strongly induced at 3 h, but their expression decreased at 1 d postactivation. *Bcl2a1d* has a role in early thymocyte survival, and it is a direct target of NF-κB (45). Its expression pattern and promoter sequences suggest that it is also a direct target of Egr-2; however, the role of Bcl2a1d in mature T cell activation is unknown. The cell survival defect in Th1 cells was not universal, because there was no Erk2-associated difference in survival or differentiation of IL-17$^+$ cells.

Under optimal conditions supporting Th2 differentiation, there was also reduced survival in the absence of Erk2, and a trend toward an increased percentage of IL-4$^+$ cells. Previous work showed that Th2 differentiation in the absence of added IL-4 is enhanced by the attenuation of Erk (10, 11, 46, 47). The dichotomy of Th1 versus Th2 differentiation was clearly illustrated by the array-expression patterns of *Tbx21* and *Gata3*, which were almost perfect mirror images of one another with respect to *Erk2* dependence and eight different conditions of activation.

The *Foxp3* locus is regulated by methylation, and a possibility is that partial demethylation, accompanying TGF-β signaling and a decrease in Dnmt1 activity, is sufficient for iTreg differentiation (25–27, 48, 49). Furthermore, pharmacological inhibition of Erk promoted Foxp3 expression and suppressor function in naive T cells, and this was also correlated with a diminished expression of *Dnmt1*, at least after 4 d of culture (12). Consistent with this, under iTreg conditions for 1 d, the array value changes associated with a loss of Erk2 were much more numerous than were those found for Th0 or Th1 conditions. Furthermore, the loss-of-Erk2 changes were overwhelmingly skewed toward increased expression. The implication is that there is suppression of gene expression, including *Foxp3*, by TGF-β that is dependent on Erk2. This would be consistent with diminished expression of the maintenance methyltransferase, Dnmt1, or possibly the de novo methyltransferase, Dnmt3b. However, neither *Dnmt1* nor *Dnmt3b* mRNA was suppressed by TGF-β at 1 d, a time when *Foxp3* has already been induced. In addition, array values and qPCR indicated that Erk2 deletion had a minimal effect on *Dnmt1* mRNA expression at 1 d compared with the magnitude of induction, although the small decrease in *Dnmt1* in *Erk2*$^{-/-}$ T cells was seen in all of the array conditions that included TGF-β. At later time points, we detected significant Erk2-dependent differences, but it is unknown whether the small Erk2-dependent differences seen at 1 d are of biological significance. We conclude that these results are not consistent with a simple model of iTreg differentiation

based entirely on the amount of *Dnmt1* mRNA expressed; but we note that the regulation of Dnmt1 activity derives from a large allosterically controlled protein complex that assembles on chromatin in a cell cycle-dependent manner (50). Independent of mRNA amount, Dnmt1 activity may be regulated in an Erk- and TGF-β–dependent manner that is not yet understood. Future studies will characterize the entire methylome of WT and *Erk2*$^{-/-}$ T cells under alternate conditions of activation and differentiation.

The set of genes that was specific to iTreg conditions and further induced in the absence of Erk2 included a number known to be part of the Treg signature, including *Foxp3* and *Nrp1*. Other genes identified in this set may suggest mechanisms of T cell differentiation, but none encodes a DNA-binding transcription factor. A separate unbiased hierarchical cluster analysis was performed, and the cluster including *Foxp3* identified an overlapping set of genes that also included three candidate transcription factors. One, *Cux1*, is a TGF-β–regulated homeobox gene that gives rise to many proteins with differing functions (51). One of the *Cux1* knockout mouse strains had multiple defects in T and B cell development; thus, we speculate that it controls part of the iTreg program (52). A second is *Stat5*, downstream of γ_C signaling and necessary for Treg function (53, 54), and a third is *Zfhx3*, Zinc finger homeobox 3, known to regulate p21$^{Cip1/Waf1}$ (55). Because Treg differentiation was shown to depend on a higher-order control that, in turn, induces *Foxp3* (32, 56–58), it is possible that these transcription factors, as well as Foxo1,3 (18, 59, 60), initiate the program of Treg gene expression.

Another mechanism of Erk2 suppression involves TGF-β signaling, a central facet of iTreg differentiation. There was an increased amount of activated p-Smad2,3 in Erk2-deficient T cells, suggesting that Erk2 attenuates the TGF-βR–mediated activation of Smads. A similar result was found for Mekk2- and Mekk3-deficient T cells, which show impaired phosphorylation of the Smad2,3 linker region, enhanced Smad transcription activity, and impaired IFN-γ production (28). In addition, Mekk3-deficient T cells were impaired in their Erk activation and were defective in their Th1 responses (61). An implication from these studies and the present work is that Mekk2,3, upstream of all of the MAPKs, are specifically acting through Erk phosphorylation to affect TGF-β signaling. A further mechanism involves Gata3, shown to be essential for Treg function (34), and in the absence of Erk2, there is a substantial increase in the expression of *Gata3* under all conditions. Finally, *Socs2* is a positive regulator of Stat3,5 signaling, and Erk2 suppresses its expression under Th0 and Th1 conditions. It is possible that, under conditions of limiting TGF-β, the signals such as those transmitted through the IL-2R are dampened by the activation of Erk2 (39). In sum, the strength of Erk2 signaling arbitrates a contingency of T cell differentiation through its role as a highly connected node in signal transduction.

An unexpected result was that the most important role for Erk2 in T cells is survival and differentiation of effector T cells, separate from its role in cell proliferation. Erk is well established as an essential signal transducer in cell cycle entry and progression in all cells previously examined and under all stimulatory conditions tested (62); yet, with the addition of costimulation through CD28, we found that T cells could still initiate cell cycle entry and complete division with a loss of *Erk2* or even a complete loss of *Erk1* and *Erk2* (data not shown). This is not congruous with studies using pharmacological inhibitors of Mek1,2, suggesting that such inhibitors have off-target effects (63). Consistent with increased division in Erk2-deficient T cells, p21$^{Cip1/Waf1}$ is strongly dependent on Erk2 for expression, making it an important pathway for negative-feedback control of T cell proliferation. This may explain, in part, the role of p21$^{Cip1/Waf1}$ in tolerance and suppression of autoimmunity (64). The mechanism underlying the bypass of Erk in T cell cycle progression is a topic of current study.

Because finely tuned Erk signaling is essential for appropriate T cell differentiation, it is perhaps not surprising that defects in Erk expression are associated with autoimmunity. Studies showed that loss of Erk activation correlated with diminished *Dnmt1* and DNA hypomethylation in patients with systemic lupus erythematosus (65, 66). From the data presented in this article, we predict increased numbers of Tregs in such patients; in one study, newly diagnosed and untreated systemic lupus erythematosus patients had increased frequencies of CD4$^+$FOXP3$^+$ T cells, which correlated positively with disease severity (67). It is unclear why an increased proportion of Tregs should correlate positively with autoimmune disease, but this is most likely correlative and not causative. Rather, changes in Erk activation underlie aberrant differentiation of T effector cells, leading to a loss of tolerance. Overall, Erk signaling is clearly pivotal in T cell differentiation and important for the regulation of T cell homeostasis.

Acknowledgments

We thank Dr. Thomas Ludwig (Columbia University, New York, NY) for providing *CreER*^{T2} mice and National Institutes of Health for class II tetramers. We also thank Dr. Ananda Goldrath and J. Adam Best for help with microarray analyses.

Disclosures

The authors have no financial conflicts of interest.

References

1. Zhu, J., and W. E. Paul. 2010. Peripheral CD4+ T-cell differentiation regulated by networks of cytokines and transcription factors. *Immunol. Rev.* 238: 247–262.
2. Yoon, S., and R. Seger. 2006. The extracellular signal-regulated kinase: multiple substrates regulate diverse cellular functions. *Growth Factors* 24: 21–44.
3. von Kriegsheim, A., D. Baiocchi, M. Birtwistle, D. Sumpton, W. Bienvenut, N. Morrice, K. Yamada, A. Lamond, G. Kalna, R. Orton, et al. 2009. Cell fate decisions are specified by the dynamic ERK interactome. *Nat. Cell Biol.* 11: 1458–1464.
4. Voisin, L., M. K. Saba-El-Leil, C. Julien, C. Frémin, and S. Meloche. 2010. Genetic demonstration of a redundant role of extracellular signal-regulated kinase 1 (ERK1) and ERK2 mitogen-activated protein kinases in promoting fibroblast proliferation. *Mol. Cell. Biol.* 30: 2918–2932.
5. Hatano, N., Y. Mori, M. Oh-hora, A. Kosugi, T. Fujikawa, N. Nakai, H. Niwa, J. Miyazaki, T. Hamaoka, and M. Ogata. 2003. Essential role for ERK2 mitogen-activated protein kinase in placental development. *Genes Cells* 8: 847–856.
6. Saba-El-Leil, M. K., F. D. Vella, B. Vernay, L. Voisin, L. Chen, N. Labrecque, S. L. Ang, and S. Meloche. 2003. An essential function of the mitogen-activated protein kinase Erk2 in mouse trophoblast development. *EMBO Rep.* 4: 964–968.
7. Yao, Y., W. Li, J. Wu, U. A. Germann, M. S. Su, K. Kuida, and D. M. Boucher. 2003. Extracellular signal-regulated kinase 2 is necessary for mesoderm differentiation. *Proc. Natl. Acad. Sci. USA* 100: 12759–12764.
8. Fischer, A. M., C. D. Katayama, G. Pagès, J. Pouysségur, and S. M. Hedrick. 2005. The role of erk1 and erk2 in multiple stages of T cell development. *Immunity* 23: 431–443.
9. Lips, D. J., O. F. Bueno, B. J. Wilkins, N. H. Purcell, R. A. Kaiser, J. N. Lorenz, L. Voisin, M. K. Saba-El-Leil, S. Meloche, J. Pouysségur, et al. 2004. MEK1-ERK2 signaling pathway protects myocardium from ischemic injury in vivo. *Circulation* 109: 1938–1941.
10. Jorritsma, P. J., J. L. Brogdon, and K. Bottomly. 2003. Role of TCR-induced extracellular signal-regulated kinase activation in the regulation of early IL-4 expression in naive CD4+ T cells. *J. Immunol.* 170: 2427–2434.
11. Yamane, H., J. Zhu, and W. E. Paul. 2005. Independent roles for IL-2 and GATA-3 in stimulating naive CD4+ T cells to generate a Th2-inducing cytokine environment. *J. Exp. Med.* 202: 793–804.
12. Luo, X., Q. Zhang, V. Liu, Z. Xia, K. L. Pothoven, and C. Lee. 2008. Cutting edge: TGF-beta-induced expression of Foxp3 in T cells is mediated through inactivation of ERK. *J. Immunol.* 180: 2757–2761.
13. Mor, A., G. Keren, Y. Kloog, and J. George. 2008. N-Ras or K-Ras inhibition increases the number and enhances the function of Foxp3 regulatory T cells. *Eur. J. Immunol.* 38: 1493–1502.
14. Pagès, G., S. Guérin, D. Grall, F. Bonino, A. Smith, F. Anjuere, P. Auberger, and J. Pouysségur. 1999. Defective thymocyte maturation in p44 MAP kinase (Erk 1) knockout mice. *Science* 286: 1374–1377.
15. Guo, K., J. E. McMinn, T. Ludwig, Y. H. Yu, G. Yang, L. Chen, D. Loh, C. Li, S. Chua, Jr., and Y. Zhang. 2007. Disruption of peripheral leptin signaling in

mice results in hyperleptinemia without associated metabolic abnormalities. *Endocrinology* 148: 3987–3997.
16. Oxenius, A., M. F. Bachmann, R. M. Zinkernagel, and H. Hengartner. 1998. Virus-specific MHC-class II-restricted TCR-transgenic mice: effects on humoral and cellular immune responses after viral infection. *Eur. J. Immunol.* 28: 390–400.
17. Ch'en, I. L., J. S. Tsau, J. D. Molkentin, M. Komatsu, and S. M. Hedrick. 2011. Mechanisms of necroptosis in T cells. *J. Exp. Med.* 208: 633–641.
18. Kerdiles, Y. M., E. L. Stone, D. R. Beisner, M. A. McGargill, I. L. Ch'en, C. Stockmann, C. D. Katayama, and S. M. Hedrick. 2010. Foxo transcription factors control regulatory T cell development and function. *Immunity* 33: 890–904.
19. McGargill, M. A., C. Choy, B. G. Wen, and S. M. Hedrick. 2008. Drak2 regulates the survival of activated T cells and is required for organ-specific autoimmune disease. *J. Immunol.* 181: 7593–7605.
20. Reich, M., T. Liefeld, J. Gould, J. Lerner, P. Tamayo, and J. P. Mesirov. 2006. GenePattern 2.0. *Nat. Genet.* 38: 500–501.
21. Saeed, A. I., N. K. Bhagabati, J. C. Braisted, W. Liang, V. Sharov, E. A. Howe, J. Li, M. Thiagarajan, J. A. White, and J. Quackenbush. 2006. TM4 microarray software suite. *Methods Enzymol.* 411: 134–193.
22. D'Souza, W. N., C. F. Chang, A. M. Fischer, M. Li, and S. M. Hedrick. 2008. The Erk2 MAPK regulates CD8 T cell proliferation and survival. *J. Immunol.* 181: 7617–7629.
23. Nekrasova, T., C. Shive, Y. Gao, K. Kawamura, R. Guardia, G. Landreth, and T. G. Forsthuber. 2005. ERK1-deficient mice show normal T cell effector function and are highly susceptible to experimental autoimmune encephalomyelitis. *J. Immunol.* 175: 2374–2380.
24. Singh, B., S. Read, C. Asseman, V. Malmström, C. Mottet, L. A. Stephens, R. Stepankova, H. Tlaskalova, and F. Powrie. 2001. Control of intestinal inflammation by regulatory T cells. *Immunol. Rev.* 182: 190–200.
25. Kim, H. P., and W. J. Leonard. 2007. CREB/ATF-dependent T cell receptor-induced FoxP3 gene expression: a role for DNA methylation. *J. Exp. Med.* 204: 1543–1551.
26. Lal, G., N. Zhang, W. van der Touw, Y. Ding, W. Ju, E. P. Bottinger, S. P. Reid, D. E. Levy, and J. S. Bromberg. 2009. Epigenetic regulation of Foxp3 expression in regulatory T cells by DNA methylation. *J. Immunol.* 182: 259–273.
27. Josefowicz, S. Z., C. B. Wilson, and A. Y. Rudensky. 2009. Cutting edge: TCR stimulation is sufficient for induction of Foxp3 expression in the absence of DNA methyltransferase 1. *J. Immunol.* 182: 6648–6652.
28. Chang, X., F. Liu, X. Wang, A. Lin, H. Zhao, and B. Su. 2011. The kinases MEKK2 and MEKK3 regulate transforming growth factor-β-mediated helper T cell differentiation. *Immunity* 34: 201–212.
29. Kim, Y., A. E. Rice, and J. M. Denu. 2003. Intramolecular dephosphorylation of ERK by MKP3. *Biochemistry* 42: 15197–15207.
30. Hannedouche, S., J. Zhang, T. Yi, W. Shen, D. Nguyen, J. P. Pereira, D. Guerini, B. U. Baumgarten, S. Roggo, B. Wen, et al. 2011. Oxysterols direct immune cell migration via EBI2. *Nature* 475: 524–527.
31. Carlson, C. M., B. T. Endrizzi, J. Wu, X. Ding, M. A. Weinreich, E. R. Walsh, M. A. Wani, J. B. Lingrel, K. A. Hogquist, and S. C. Jameson. 2006. Kruppel-like factor 2 regulates thymocyte and T-cell migration. *Nature* 442: 299–302.
32. Sugimoto, N., T. Oida, K. Hirota, K. Nakamura, T. Nomura, T. Uchiyama, and S. Sakaguchi. 2006. Foxp3-dependent and -independent molecules specific for CD25+CD4+ natural regulatory T cells revealed by DNA microarray analysis. *Int. Immunol.* 18: 1197–1209.
33. Kitamura, K., J. M. Farber, and B. L. Kelsall. 2010. CCR6 marks regulatory T cells as a colon-tropic, IL-10-producing phenotype. *J. Immunol.* 185: 3295–3304.
34. Wang, Y., M. A. Su, and Y. Y. Wan. 2011. An essential role of the transcription factor GATA-3 for the function of regulatory T cells. *Immunity* 35: 337–348.
35. Oestreich, K. J., and A. S. Weinmann. 2012. T-bet employs diverse regulatory mechanisms to repress transcription. *Trends Immunol.* 33: 78–83.
36. Zhu, J., H. Yamane, and W. E. Paul. 2010. Differentiation of effector CD4 T cell populations (*). *Annu. Rev. Immunol.* 28: 445–489.
37. Feuerer, M., J. A. Hill, K. Kretschmer, H. von Boehmer, D. Mathis, and C. Benoist. 2010. Genomic definition of multiple ex vivo regulatory T cell subphenotypes. *Proc. Natl. Acad. Sci. USA* 107: 5919–5924.
38. Balomenos, D., J. Martín-Caballero, M. I. García, I. Prieto, J. M. Flores, M. Serrano, and C. Martínez-A. 2000. The cell cycle inhibitor p21 controls T-cell proliferation and sex-linked lupus development. *Nat. Med.* 6: 171–176.
39. Tannahill, G. M., J. Elliott, A. C. Barry, L. Hibbert, N. A. Cacalano, and J. A. Johnston. 2005. SOCS2 can enhance interleukin-2 (IL-2) and IL-3 signaling by accelerating SOCS3 degradation. *Mol. Cell. Biol.* 25: 9115–9126.
40. Islam, S. A., D. S. Chang, R. A. Colvin, M. H. Byrne, M. L. McCully, B. Moser, S. A. Lira, I. F. Charo, and A. D. Luster. 2011. Mouse CCL8, a CCR8 agonist, promotes atopic dermatitis by recruiting IL-5+ T(H)2 cells. *Nat. Immunol.* 12: 167–177.
41. Constant, S. L., and K. Bottomly. 1997. Induction of Th1 and Th2 CD4+ T cell responses: the alternative approaches. *Annu. Rev. Immunol.* 15: 297–322.
42. Iborra, S., M. Soto, L. Stark-Aroeira, E. Castellano, B. Alarcón, C. Alonso, E. Santos, and E. Fernández-Malavé. 2011. H-ras and N-ras are dispensable for T-cell development and activation but critical for protective Th1 immunity. *Blood* 117: 5102–5111.
43. Youle, R. J., and A. Strasser. 2008. The BCL-2 protein family: opposing activities that mediate cell death. *Nat. Rev. Mol. Cell Biol.* 9: 47–59.
44. Boise, L. H., A. R. Gottschalk, J. Quintáns, and C. B. Thompson. 1995. Bcl-2 and Bcl-2-related proteins in apoptosis regulation. *Curr. Top. Microbiol. Immunol.* 200: 107–121.
45. Mandal, M., C. Borowski, T. Palomero, A. A. Ferrando, P. Oberdoerffer, F. Meng, A. Ruiz-Vela, M. Ciofani, J. C. Zuniga-Pflucker, I. Screpanti, et al. 2005. The BCL2A1 gene as a pre-T cell receptor-induced regulator of thymocyte survival. *J. Exp. Med.* 201: 603–614.
46. Leitenberg, D., and K. Bottomly. 1999. Regulation of naive T cell differentiation by varying the potency of TCR signal transduction. *Semin. Immunol.* 11: 283–292.
47. Zhu, J., and W. E. Paul. 2008. CD4 T cells: fates, functions, and faults. *Blood* 112: 1557–1569.
48. Floess, S., J. Freyer, C. Siewert, U. Baron, S. Olek, J. Polansky, K. Schlawe, H. D. Chang, T. Bopp, E. Schmitt, et al. 2007. Epigenetic control of the foxp3 locus in regulatory T cells. *PLoS Biol.* 5: e38.
49. Polansky, J. K., K. Kretschmer, J. Freyer, S. Floess, A. Garbe, U. Baron, S. Olek, A. Hamann, H. von Boehmer, and J. Huehn. 2008. DNA methylation controls Foxp3 gene expression. *Eur. J. Immunol.* 38: 1654–1663.
50. Jurkowska, R. Z., T. P. Jurkowski, and A. Jeltsch. 2011. Structure and function of mammalian DNA methyltransferases. *ChemBioChem* 12: 206–222.
51. Sansregret, L., and A. Nepveu. 2008. The multiple roles of CUX1: insights from mouse models and cell-based assays. *Gene* 412: 84–94.
52. Sinclair, A. M., J. A. Lee, A. Goldstein, D. Xing, S. Liu, R. Ju, P. W. Tucker, E. J. Neufeld, and R. H. Scheuermann. 2001. Lymphoid apoptosis and myeloid hyperplasia in CCAAT displacement protein mutant mice. *Blood* 98: 3658–3667.
53. Cohen, A. C., K. C. Nadeau, W. Tu, V. Hwa, K. Dionis, L. Bezrodnik, A. Teper, M. Gaillard, J. Heinrich, A. M. Krensky, et al. 2006. Cutting edge: Decreased accumulation and regulatory function of CD4+ CD25(high) T cells in human STAT5b deficiency. *J. Immunol.* 177: 2770–2774.
54. Burchill, M. A., J. Yang, C. Vogtenhuber, B. R. Blazar, and M. A. Farrar. 2007. IL-2 receptor beta-dependent STAT5 activation is required for the development of Foxp3+ regulatory T cells. *J. Immunol.* 178: 280–290.
55. Mabuchi, M., H. Kataoka, Y. Miura, T. S. Kim, M. Kawaguchi, M. Ebi, M. Tanaka, Y. Mori, E. Kubota, T. Mizushima, et al. 2010. Tumor suppressor, AT motif binding factor 1 (ATBF1), translocates to the nucleus with runt domain transcription factor 3 (RUNX3) in response to TGF-beta signal transduction. *Biochem. Biophys. Res. Commun.* 398: 321–325.
56. Gavin, M. A., J. P. Rasmussen, J. D. Fontenot, V. Vasta, V. C. Manganiello, J. A. Beavo, and A. Y. Rudensky. 2007. Foxp3-dependent programme of regulatory T-cell differentiation. *Nature* 445: 771–775.
57. Lin, W., D. Haribhai, L. M. Relland, N. Truong, M. R. Carlson, C. B. Williams, and T. A. Chatila. 2007. Regulatory T cell development in the absence of functional Foxp3. *Nat. Immunol.* 8: 359–368.
58. Hill, J. A., M. Feuerer, K. Tash, S. Haxhinasto, J. Perez, R. Melamed, D. Mathis, and C. Benoist. 2007. Foxp3 transcription-factor-dependent and -independent regulation of the regulatory T cell transcriptional signature. *Immunity* 27: 786–800.
59. Ouyang, W., O. Beckett, Q. Ma, J. H. Paik, R. A. DePinho, and M. O. Li. 2010. Foxo proteins cooperatively control the differentiation of Foxp3+ regulatory T cells. *Nat. Immunol.* 11: 618–627.
60. Harada, Y., Y. Harada, C. Elly, G. Ying, J. H. Paik, R. A. DePinho, and Y. C. Liu. 2010. Transcription factors Foxo3a and Foxo1 couple the E3 ligase Cbl-b to the induction of Foxp3 expression in induced regulatory T cells. *J. Exp. Med.* 207: 1381–1391.
61. Wang, X., F. Zhang, F. Chen, D. Liu, Y. Zheng, Y. Zhang, C. Dong, and B. Su. 2011. MEKK3 regulates IFN-gamma production in T cells through the Rac1/2-dependent MAPK cascades. *J. Immunol.* 186: 5791–5800.
62. Meloche, S., and J. Pouysségur. 2007. The ERK1/2 mitogen-activated protein kinase pathway as a master regulator of the G1- to S-phase transition. *Oncogene* 26: 3227–3239.
63. Appleman, L. J., A. A. van Puijenbroek, K. M. Shu, L. M. Nadler, and V. A. Boussiotis. 2002. CD28 costimulation mediates down-regulation of p27kip1 and cell cycle progression by activation of the PI3K/PKB signaling pathway in primary human T cells. *J. Immunol.* 168: 2729–2736.
64. Zhu, B., A. L. Symonds, J. E. Martin, D. Kioussis, D. C. Wraith, S. Li, and P. Wang. 2008. Early growth response gene 2 (Egr-2) controls the self-tolerance of T cells and prevents the development of lupuslike autoimmune disease. *J. Exp. Med.* 205: 2295–2307.
65. Renaudineau, Y., and P. Youinou. 2011. Epigenetics and autoimmunity, with special emphasis on methylation. *Keio J. Med.* 60: 10–16.
66. Javierre, B. M., and B. Richardson. 2011. A new epigenetic challenge: systemic lupus erythematosus. *Adv. Exp. Med. Biol.* 711: 117–136.
67. Liu, Y., T. Zhu, G. Cai, Y. Qin, W. Wang, G. Tang, D. Zhao, and Q. Shen. 2011. Elevated circulating CD4+ ICOS+ Foxp3+ T cells contribute to overproduction of IL-10 and are correlated with disease severity in patients with systemic lupus erythematosus. *Lupus* 20: 620–627.